

Electronic Supplementary Material

Interface-modulated fabrication of hierarchical yolk–shell $\text{Co}_3\text{O}_4/\text{C}$ dodecahedrons as stable anodes for lithium and sodium storage

Yuzhu Wu^{1,§}, Jiashen Meng^{1,§}, Qi Li¹ (✉), Chaojiang Niu¹, Xuanpeng Wang¹, Wei Yang¹, Wei Li¹, and Liqiang Mai^{1,2} (✉)

¹ State Key Laboratory of Advanced Technology for Materials Synthesis and Processing, Wuhan University of Technology, Wuhan 430070, China

² Department of Chemistry, University of California, Berkeley, California 94720, USA

[§] These authors contributed equally to this work.

Supporting information to DOI 10.1007/s12274-017-1433-6

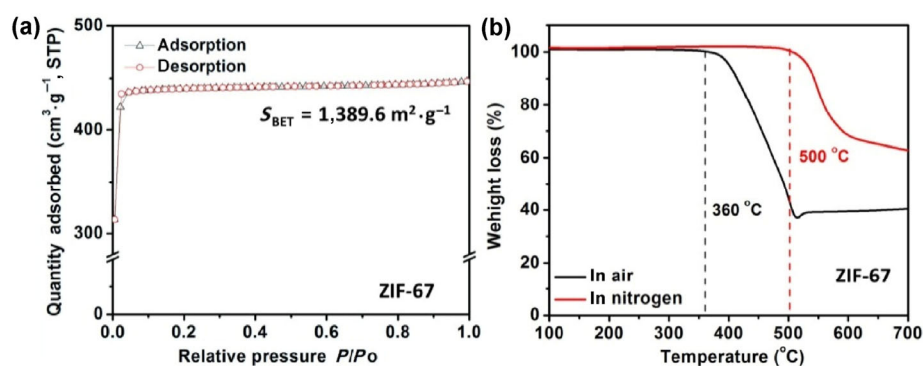


Figure S1 (a) N_2 adsorption/desorption isotherm curve of the as-synthesized rhombic dodecahedral morphology ZIF-67. (b) TG curves of ZIF-67 in air (black) and nitrogen (red) atmosphere.

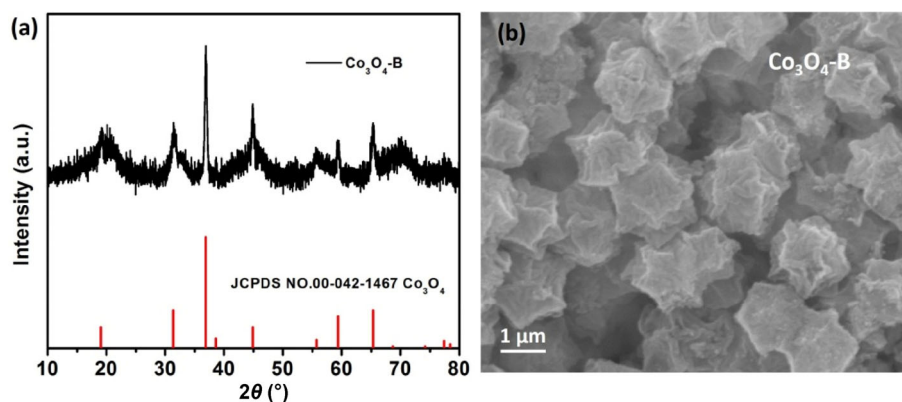


Figure S2 XRD pattern (a) and SEM image of Co_3O_4 bulks (denoted as $\text{Co}_3\text{O}_4\text{-B}$).

Address correspondence to Liqiang Mai, mlq518@whut.edu.cn; Qi Li, qi.li@whut.edu.cn

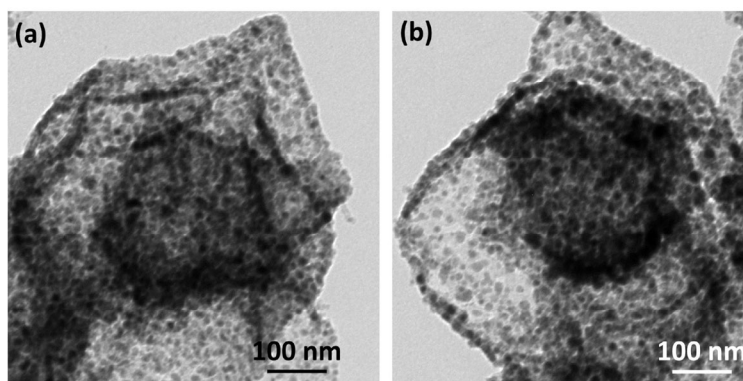


Figure S3 TEM images of the yolk-shell $\text{Co}_3\text{O}_4/\text{C}$ dodecahedrons.

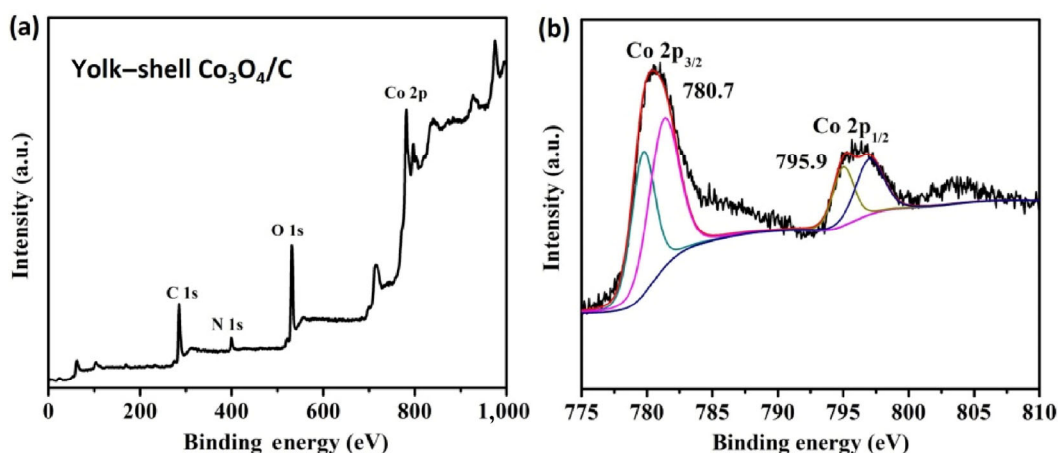


Figure S4 XPS survey spectra of the yolk-shell $\text{Co}_3\text{O}_4/\text{C}$ dodecahedrons: (a) wide scan of $\text{Co}_3\text{O}_4/\text{C}$, (b) Co 2p.

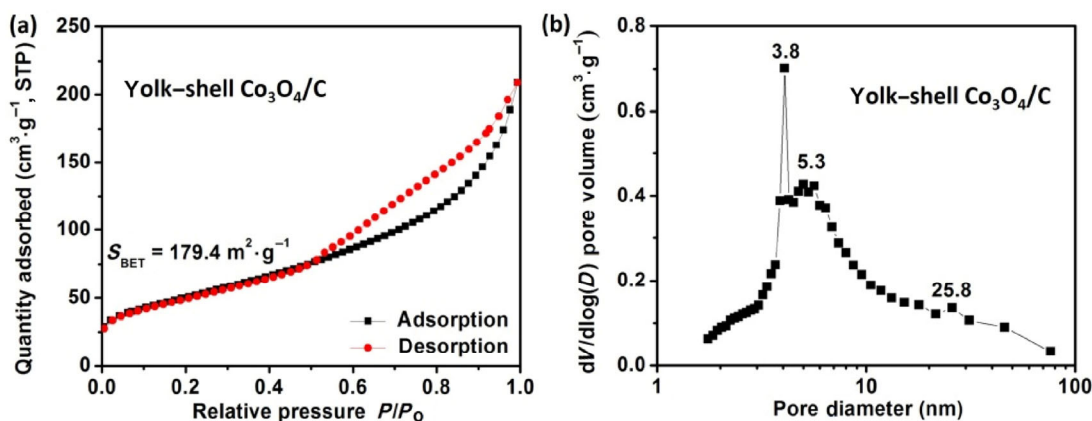


Figure S5 (a) N_2 adsorption/desorption isotherm curve and (b) pore size distribution of the yolk-shell $\text{Co}_3\text{O}_4/\text{C}$ dodecahedrons.

MOFs are formed by linking organic and inorganic moieties through coordination bonding. ZIFs belong to a subclass of MOFs materials, whose skeleton structures are made of metal ions and imidazoles organic ligands by coordination polymerization. Because of the inherent structure of ZIF-67, it has high specific surface area and high porosity. But after the pyrolysis of ZIF-67, its inherent porous channel structure will collapse, leading to the smaller specific surface area of $\text{Co}_3\text{O}_4/\text{C}$ dodecahedrons than that of ZIF-67.

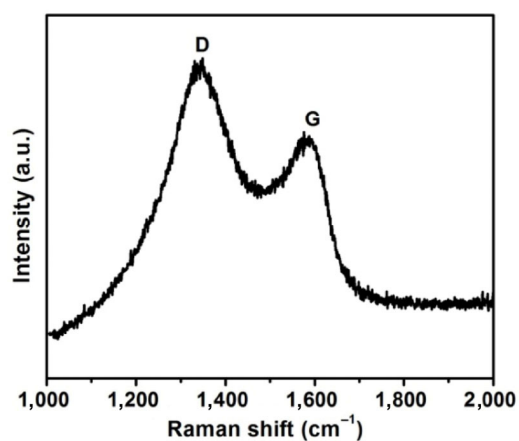


Figure S6 Raman spectrum of the yolk-shell $\text{Co}_3\text{O}_4/\text{C}$ dodecahedrons, showing the amorphous nature of carbon in $\text{Co}_3\text{O}_4/\text{C}$ dodecahedrons.

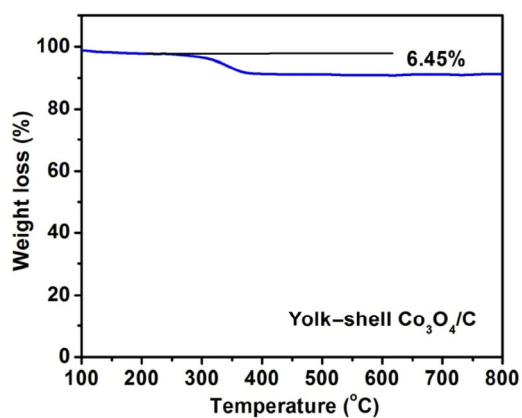


Figure S7 TG curve of the yolk-shell $\text{Co}_3\text{O}_4/\text{C}$ dodecahedrons in air. The mass content of carbon in the yolk-shell $\text{Co}_3\text{O}_4/\text{C}$ is about 6.45 wt.%.

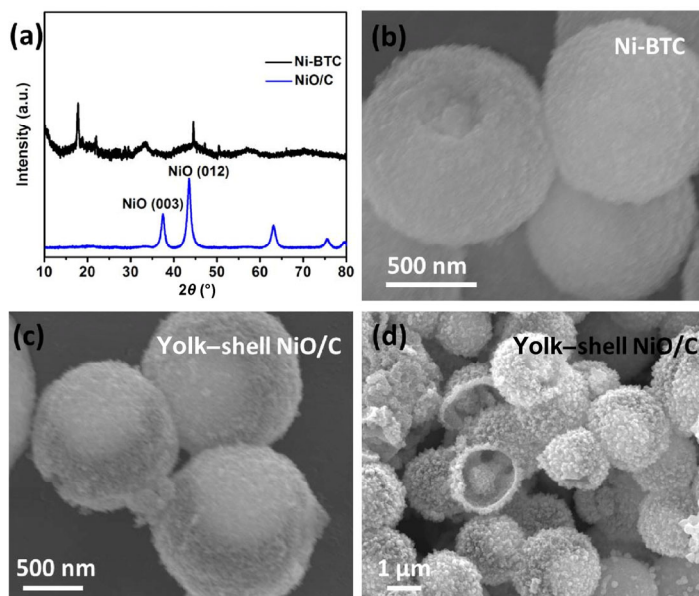


Figure S8 (a) XRD patterns of the as-synthesized Ni-BTC and yolk-shell NiO/C microspheres. (b) SEM image of the as-synthesized Ni-BTC microspheres. ((c) and (d)) SEM images of the yolk-shell NiO/C microspheres.

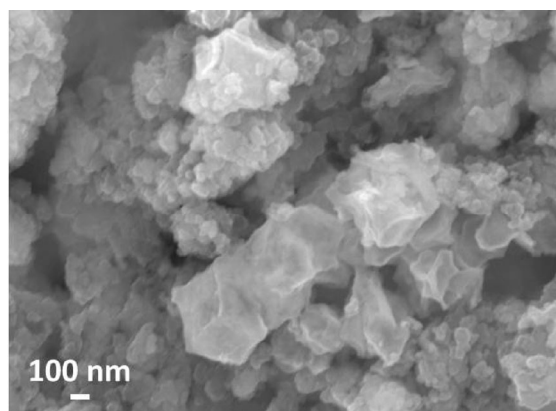


Figure S9 SEM image of the $\text{Co}_3\text{O}_4/\text{C}$ dodecahedrons after cycling at $200 \text{ mA}\cdot\text{g}^{-1}$ for 50 cycles, showing no notable variation in morphology. It should be noted that the small nanoparticles observed in the image are carbon black.

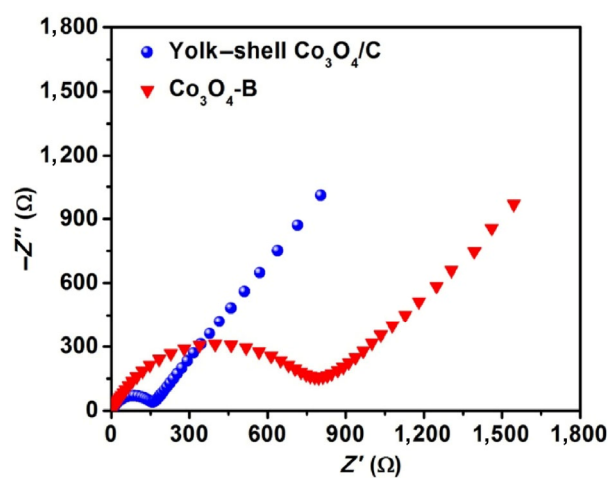


Figure S10 Electrochemical impedance spectra (Nyquist plots) of the yolk-shell $\text{Co}_3\text{O}_4/\text{C}$ dodecahedrons and $\text{Co}_3\text{O}_4\text{-B}$.

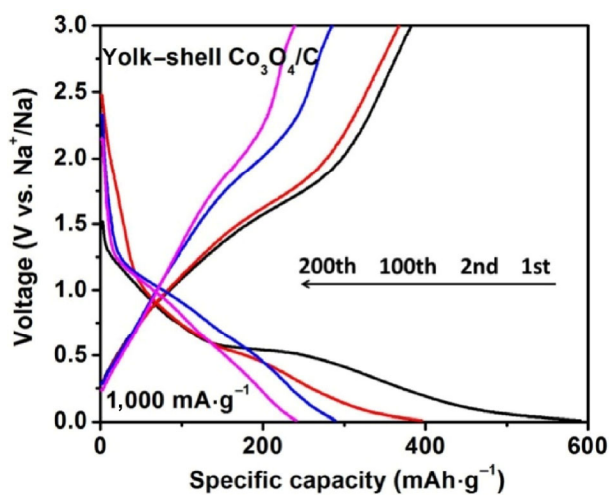


Figure S11 Electrochemical performance of yolk-shell $\text{Co}_3\text{O}_4/\text{C}$ dodecahedrons in SIBs: galvanostatic charge/discharge profiles at a current density of $1,000 \text{ mA}\cdot\text{g}^{-1}$.

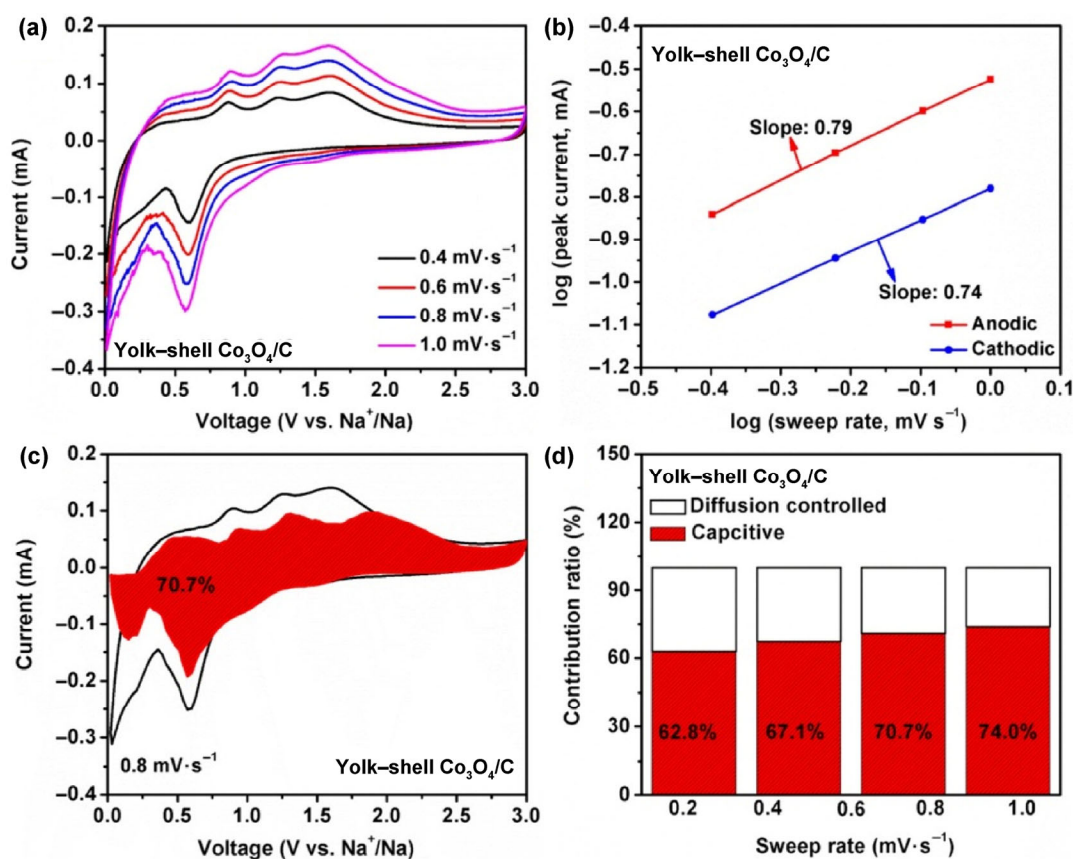


Figure S12 Kinetic analysis of the electrochemical behavior vs. Na^+/Na for the yolk-shell $\text{Co}_3\text{O}_4/\text{C}$ dodecahedrons. (a) CV curves at various scan rates from 0.2 to 1.0 $\text{mV}\cdot\text{s}^{-1}$. (b) Determination of the b -value using the relationship between peak current and scan rate. (c) Separation of the capacitive and diffusion currents at a scan rate of 0.8 $\text{mV}\cdot\text{s}^{-1}$. (d) Contribution ratio of the capacitive and diffusion-controlled charge at various scan rates.

Table S1 Comparison of the cycling performance for LIBs with previous reports

	Current density ($\text{mA}\cdot\text{g}^{-1}$)	Specific capacity ($\text{mA}\cdot\text{g}^{-1}$)	Cycle number	Reference
Yolk-shell $\text{Co}_3\text{O}_4/\text{C}$ dodecahedrons	200	1,100	120	This work
Co_3O_4 nanocages	50	970	30	[S1]
Co_3O_4 polyhedra/MWCNTs	100	889	100	[S2]
Co_3O_4 embedded N-porous carbon dodecahedrons	100	1,350	100	[S3]
Ultrafine Co_3O_4 nanocrystallites in grapheme oxide	200	908	100	[S4]

Table S2 Comparison of the cycling performance for SIBs with previous reports

	Current density ($\text{mA}\cdot\text{g}^{-1}$)	Specific capacity ($\text{mA}\cdot\text{g}^{-1}$)	Cycle number	Reference
Yolk-shell $\text{Co}_3\text{O}_4/\text{C}$ dodecahedrons	1,000	240	200	This work
$\text{Co}_3\text{O}_4@\text{CNTs}$	160	440	30	[S5]
Nanostructured Co_3O_4	25	447	50	[S6]
Co_3O_4 MNSs @ 3DGNs	25	523	50	[S7]
m- Co_3O_4	90	416	100	[S8]

References

- [S1] Jiang, Z.; Li, Z. P.; Qin, Z. H.; Sun, H. Y.; Jiao, X. L.; Chen, D. R. LDH nanocages synthesized with MOF templates and their high performance as supercapacitors. *Nanoscale* **2013**, *5*, 11770–11775.
- [S2] Li, W. Y.; Xu, L. N.; Chen, J. Co₃O₄ nanomaterials in lithium-ion batteries and gas sensors. *Adv. Funct. Mater.* **2005**, *15*, 851–857.
- [S3] Du, N.; Zhang, H.; Chen, B. D.; Wu, J. B.; Ma, X. Y.; Liu, Z. H.; Zhang, Y. Q.; Yang, D. R.; Huang, X. H.; Tu, J. P. Porous Co₃O₄ nanotubes derived from Co₄(CO)₁₂ clusters on carbon nanotube templates: A highly efficient material for Li-battery applications. *Adv. Mater.* **2007**, *19*, 4505–4509.
- [S4] Huang, G.; Zhang, F. F.; Du, X. C.; Qin, Y. L.; Yin, D. M.; Wang, L. M. Metal organic frameworks route to *in situ* insertion of multiwalled carbon nanotubes in Co₃O₄ polyhedra as anode materials for lithium-ion batteries. *ACS Nano* **2015**, *9*, 1592–1599.
- [S5] Li, S.; Qiu, J. X.; Lai, C.; Ling, M.; Zhao, H. J.; Zhang, S. Q. Surface capacitive contributions: Towards high rate anode materials for sodium ion batteries. *Nano Energy* **2015**, *12*, 224–230.
- [S6] Zhao, K. N.; Liu, F. N.; Niu, C. J.; Xu, W. W.; Dong, Y. F.; Zhang, L.; Xie, S. M.; Yan, M. Y.; Wei, Q. L.; Zhao, D. Y. et al. Graphene oxide wrapped amorphous copper vanadium oxide with enhanced capacitive behavior for high-rate and long-life lithium-ion battery anodes. *Adv. Sci.* **2015**, *2*, 1500154.
- [S7] Rahman, M. M.; Glushenkov, A. M.; Ramireddy, T.; Chen, Y. Electrochemical investigation of sodium reactivity with nanostructured Co₃O₄ for sodium-ion batteries. *Chem. Commun.* **2014**, *50*, 5057–5060.
- [S8] Jian, Z. L.; Liu, P.; Li, F. J.; Chen, M. W.; Zhou, H. S. Monodispersed hierarchical Co₃O₄ spheres intertwined with carbon nanotubes for use as anode materials in sodium-ion batteries. *J. Mater. Chem. A* **2014**, *2*, 13805–13809.